Time-Domain Description of the SFG Spectroscopy

Journal Club

2015.10.02

Zaure

The excitation of an ensemble of molecules by fs IR pulse which creates a transient first-order polarization $P^{(1)}(t)$.

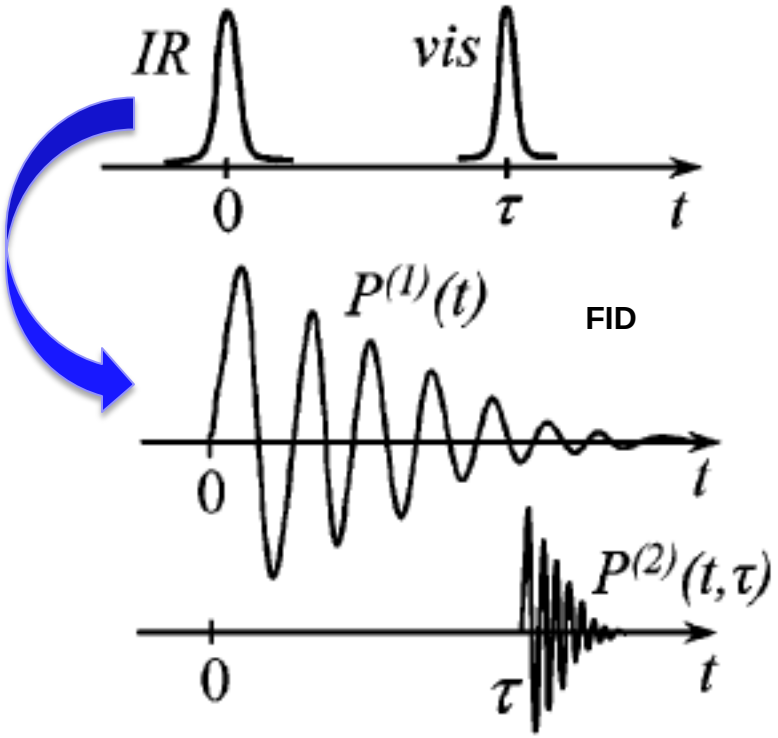

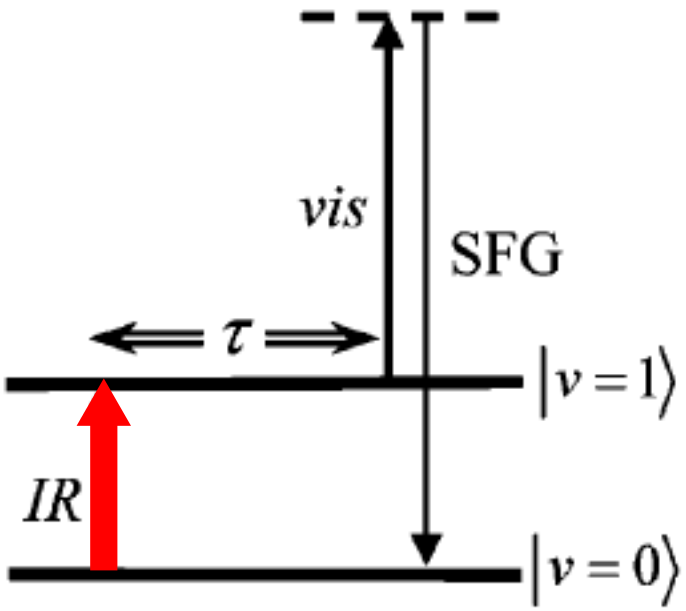

$$P^{(1)}(t) = \int_0^\infty dt_1\, R(t_1) E_{IR}(t - t_1) = R(t) \otimes E_{IR}(t)$$

R- molecular response function

Benderskii 2005

This $P^{(1)}(t)$ via optical upconversion with the overlapping VIS pulse (non-resonant) gives rise to $P^{(2)}(t)$, oscillating at a frequency that is the sum of the infrared and the visible frequencies.

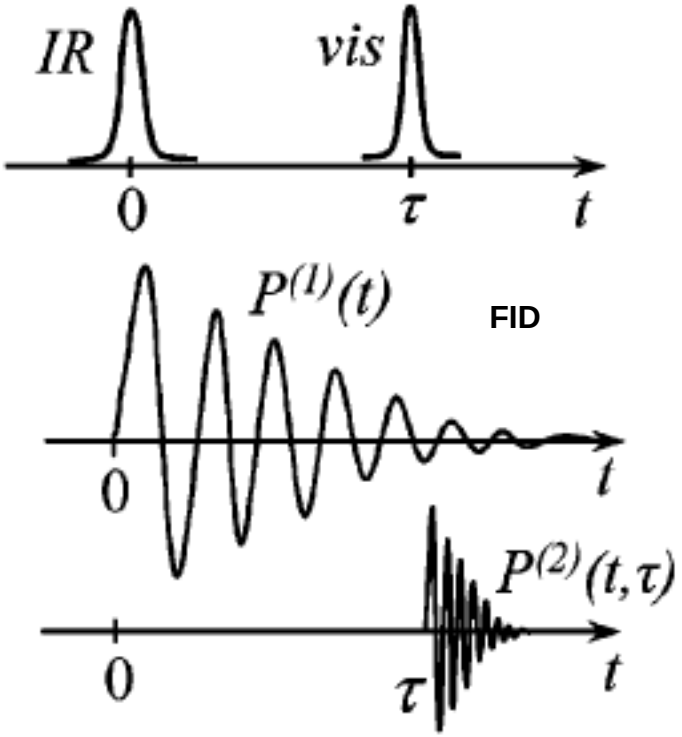

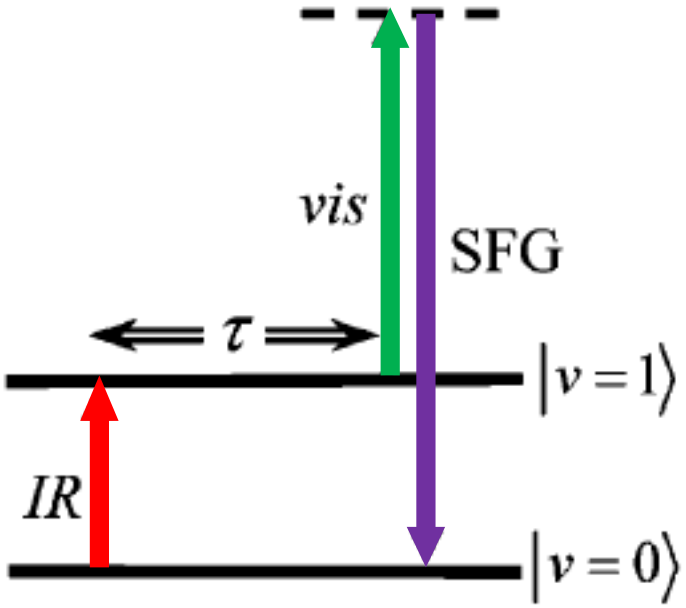

$$P^{(2)}(t;\tau) \propto E_{SFG}(t;\tau)$$

Benderskii 2005

$$E_{SFG}(t;\tau) = \int_0^\infty dt_2 \int_0^\infty dt_1 \, R^{(2)}(t_2, t_1; \tau) E_{vis}(t - t_2) E_{IR}(t - t_2 - t_1)$$

- $R^{(2)}(t_1, t_2) \approx R(t_1)\delta(t_2)$ (approximation)
- $P^{(1)}(t) = \int_0^\infty dt_1 \, R(t_1) E_{IR}(t - t_1) = R(t) \otimes E_{IR}(t)$ (convolution)

$$E_{SFG}(t;\tau) = E_{vis}(t;\tau) \int_0^\infty dt_1 \, R(t_1) E_{IR}(t - t_1) = [R(t) \otimes E_{IR}(t)] E_{vis}(t;\tau)$$

$$I_{SFG-FID}(\tau) \propto \int_{-\infty}^{+\infty} |E_{SFG}(t,\tau)|^2 dt$$

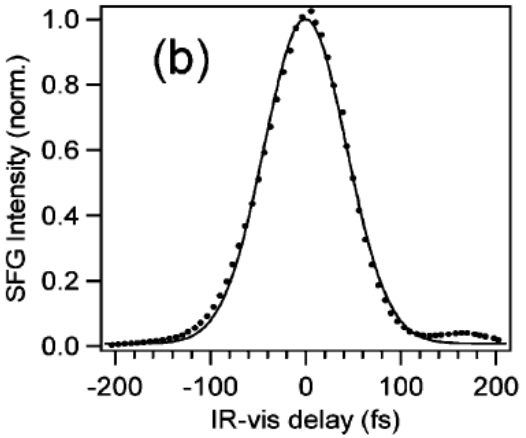

Fourier transformation:

$$E_{SFG}(t,\tau) \Rightarrow \tilde{E}_{SFG}(\omega,\tau)$$

$$\tilde{E}_{SFG}(\omega,\tau) \propto \int_{-\infty}^{+\infty} E_{SFG}(t,\tau)e^{i\omega t}dt = \int_{-\infty}^{+\infty} [R(t) \otimes E_{IR}(t)]E_{vis}(t,\tau)e^{i\omega t}dt$$

$$= [\tilde{R}(\omega)\tilde{E}_{IR}(\omega)] \otimes \tilde{E}_{vis}(\omega,\tau)$$

$$I_{SFG}(\omega,\tau) \propto \left|\tilde{E}_{SFG}(\omega,\tau)\right|^2$$

Time-Domain SFG Spectroscopy Using Mid-IR Pulse Shaping: Practical and Intrinsic Advantages

Jennifer E. Laaser, Wei Xiong, and Martin T. Zanni
J. Phys. Chem. B 2011, 115, 2536–2546

PDI Monolayer on Gold

Time-domain approach for SFG spectroscopy produces spectra that are much more accurate

1,4-phenylene diisocyanide (PDI) on gold

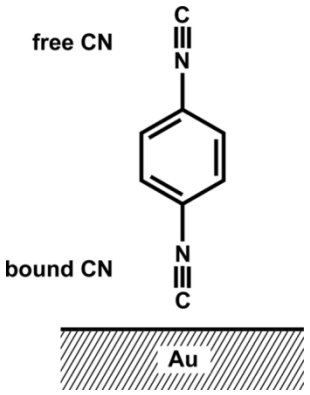

The conjugated ring structure facilitates electron transfer, the two CN groups allow contact with two metal electrodes, and the electronic coupling to the metal is stronger than for comparable thiol compounds, providing a lower barrier to electron transport. One important property of PDI is the structural heterogeneity with which it binds to the metal surface, because the binding mode will influence the electronic coupling strength between the molecular electronic orbitals and the metal surface.

Shaper-based Phase-stable Heterodyned SFG

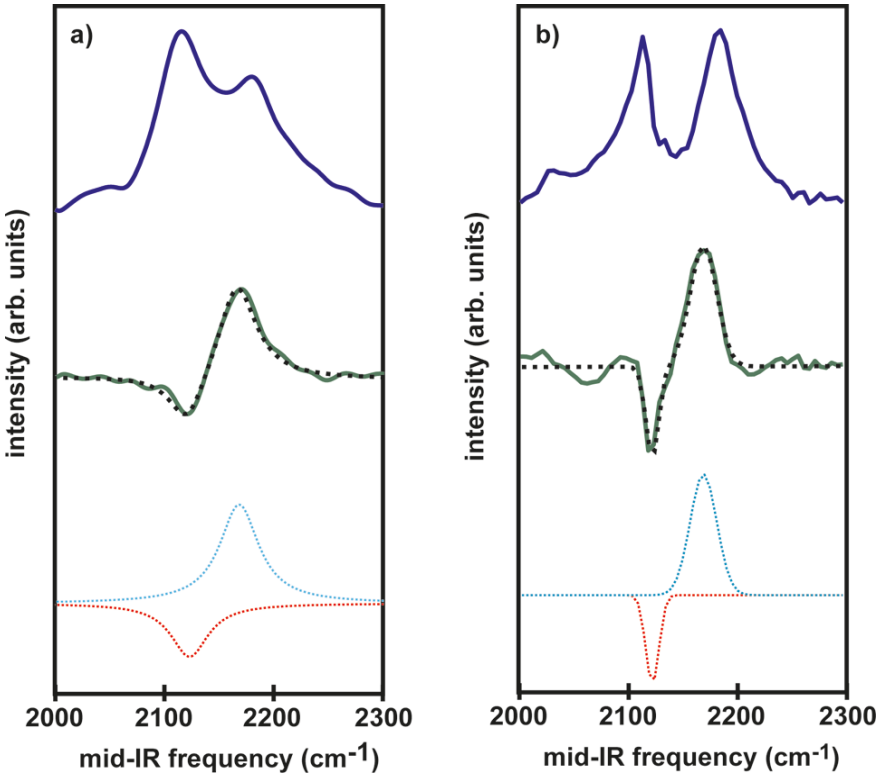

frequency-domain technique

time-domain technique

Shaper-based Phase-stable Heterodyned SFG

800 nm Ti:sapphire laser output split: mid-IR and visible pulses

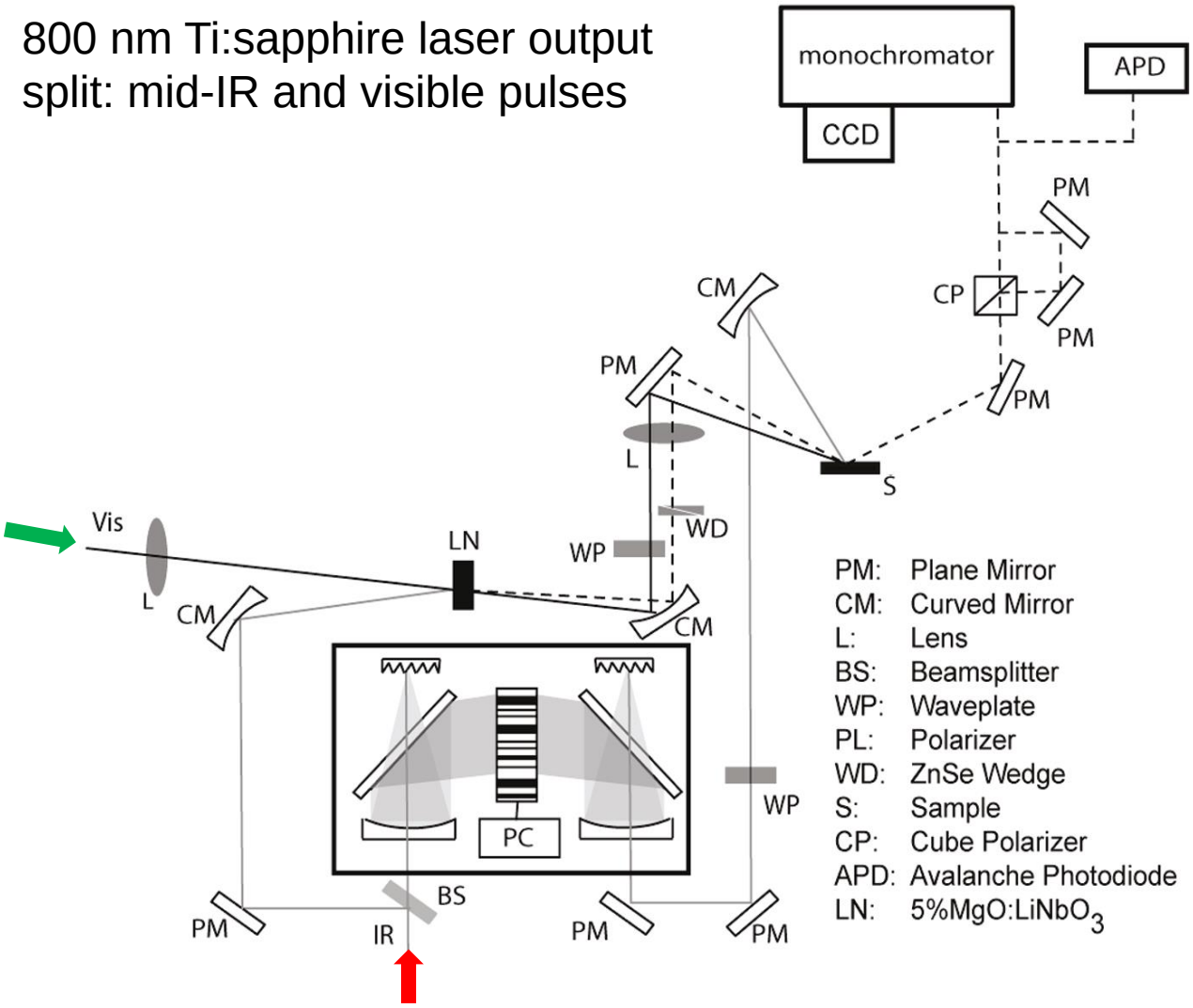

Visible Beam

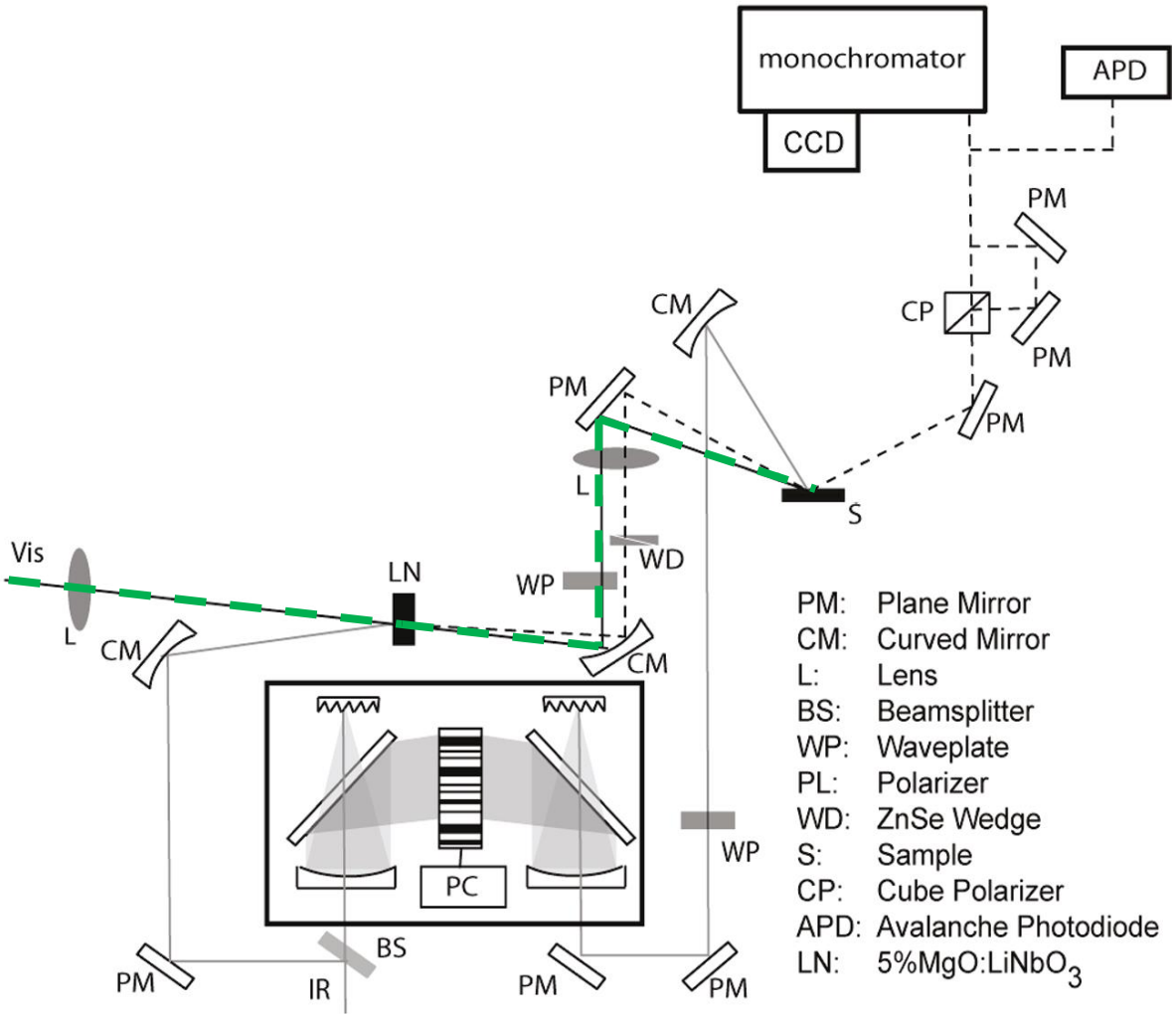

mid-IR

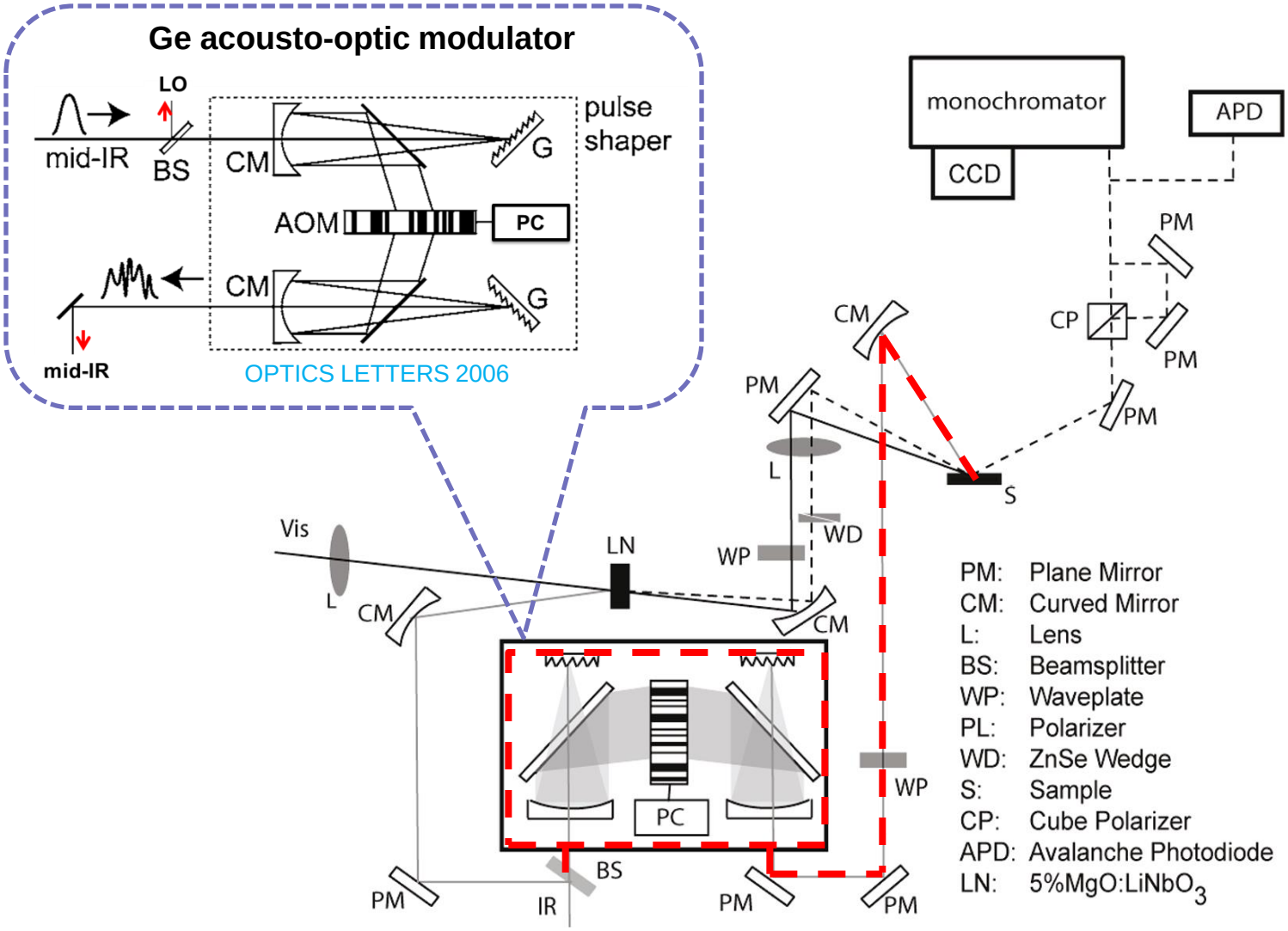
Ge acousto-optic modulator
LO
mid-IR
BS
CM
G
pulse shaper
AOM
PC
CM
G
mid-IR
OPTICS LETTERS 2006
monochromator
CCD
APD
PM
CP
PM
PM
CM
PM
L
S
WD
Vis
LN
WP
L
CM
CM
PC
WP
BS
PM
IR
PM
PM
PM: Plane Mirror
CM: Curved Mirror
L: Lens
BS: Beamsplitter
WP: Waveplate
PL: Polarizer
WD: ZnSe Wedge
S: Sample
CP: Cube Polarizer
APD: Avalanche Photodiode
LN: 5%MgO:LiNbO3

Local Oscillator Generation

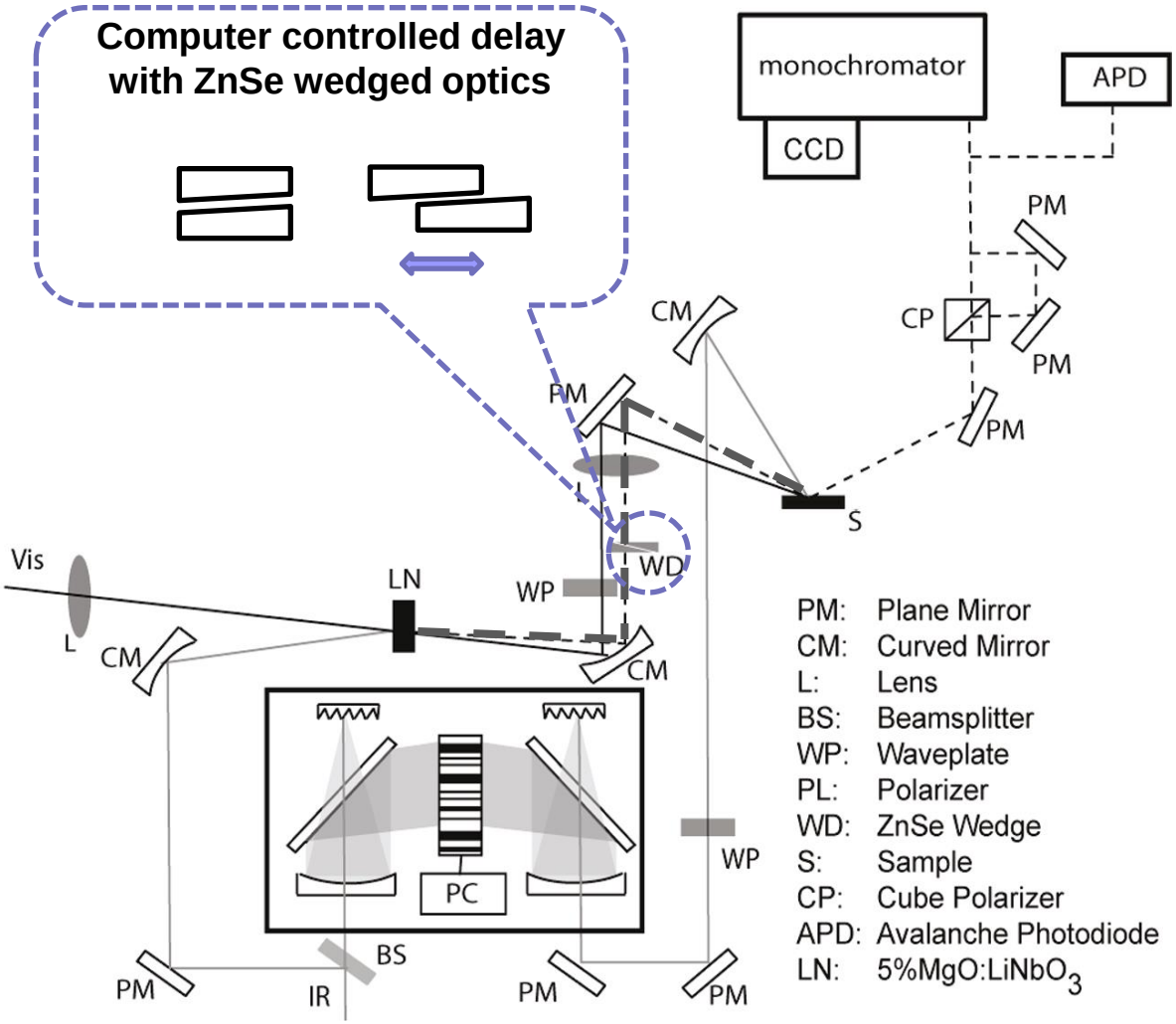

Data Processing: Frequency-domain

$$I_{het}(\omega) \approx 2Re[E_{SFG}(\omega)^* E_{LO}(\omega)]$$
$$\propto 2Re[E_{vis}(\omega) \otimes R(\omega)]$$

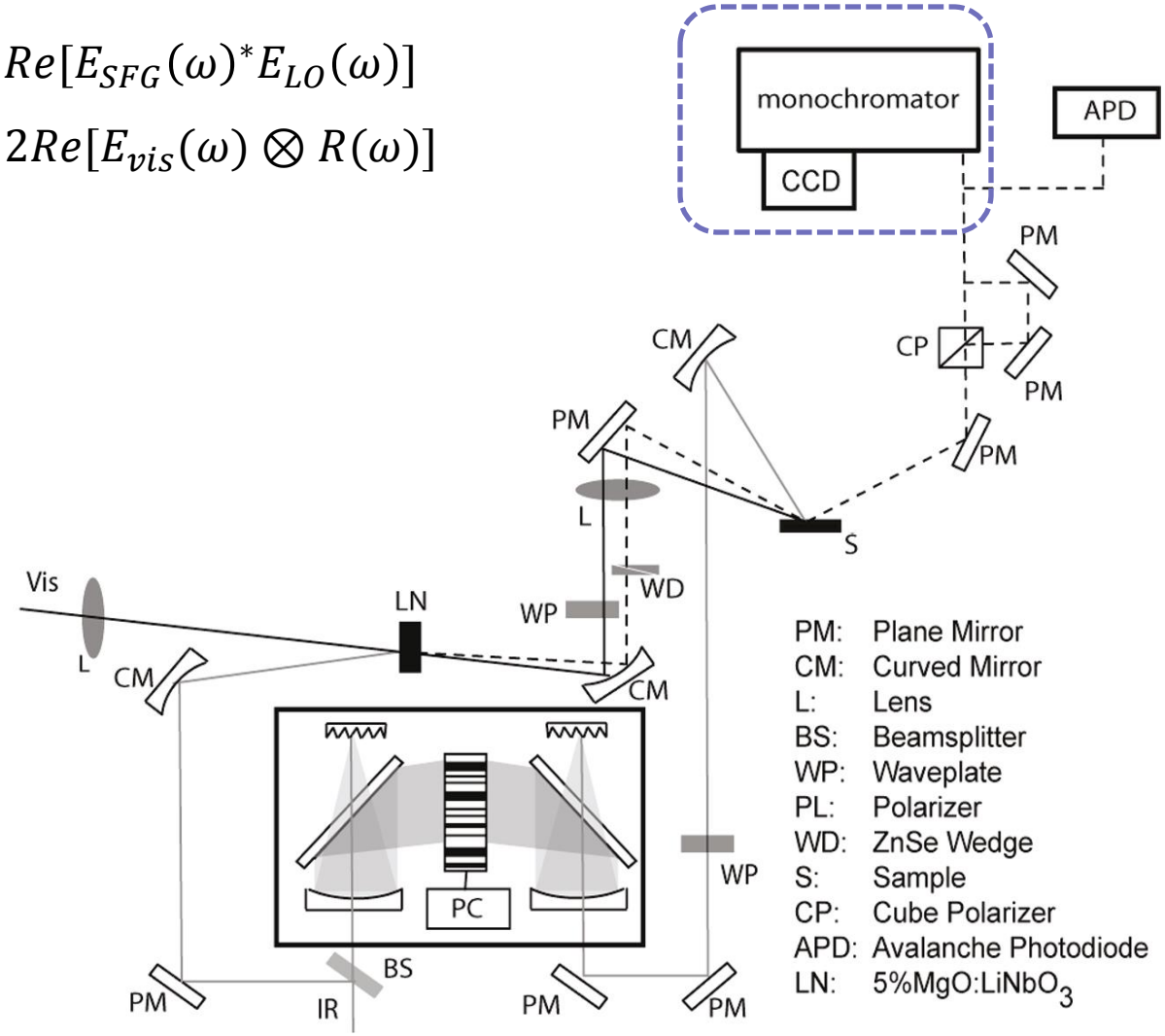

Data Processing: Time-domain

$$I_{het}(\tau) \approx 2Re\{[E_{SFG}{}^{*}E_{LO}](\tau)\} \propto 2Re\{R(\tau)\}$$

switching from the grating to a mirror

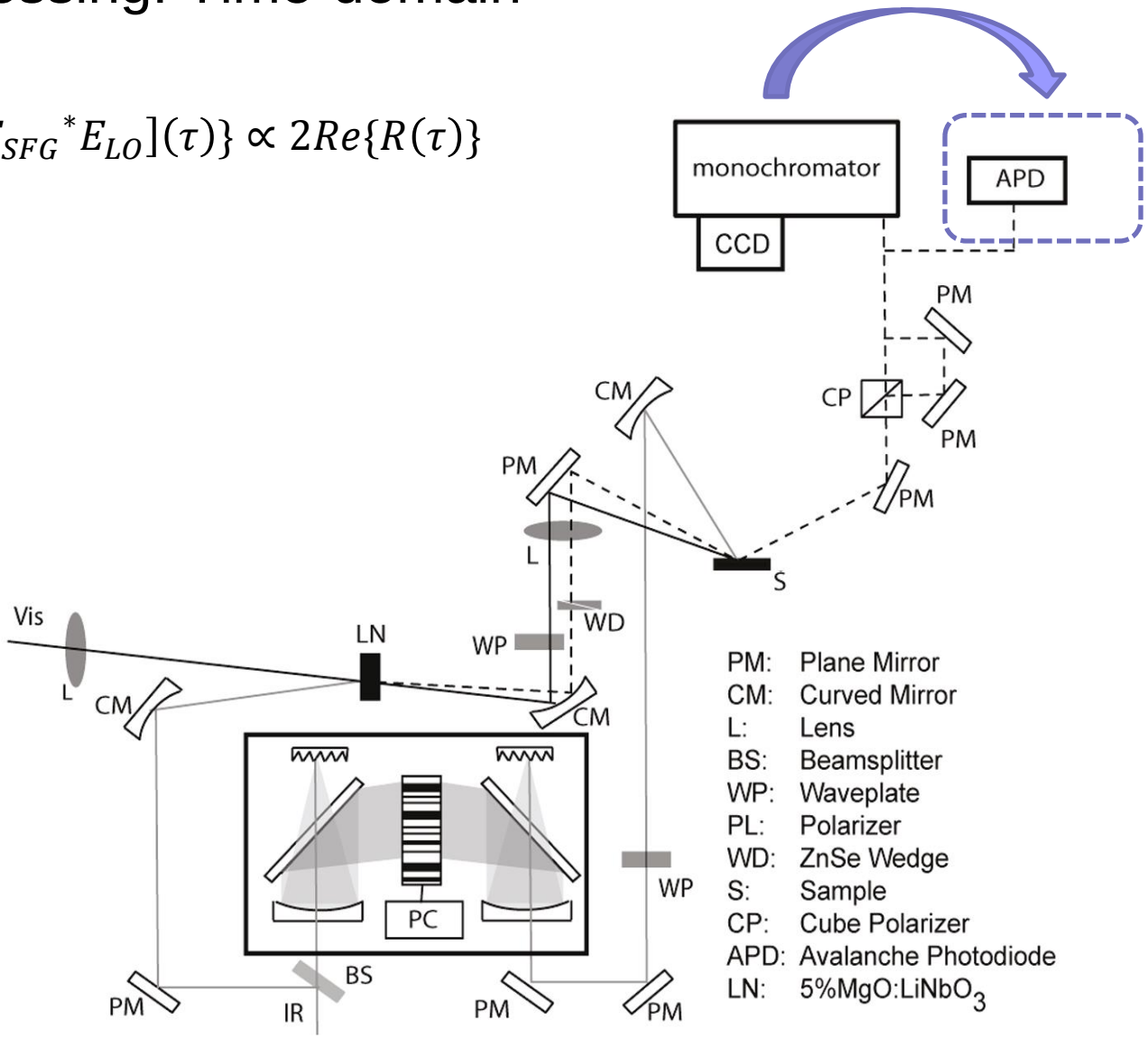

Phase Stability

- LO and vis pulses follow nearly the same path btw the $LiNbO_3$ (LN) crystal and the sample.
- LO through ZnSe wedges provides highly accurate time delays and no phase drift!
- Phase drift of only 1.5^o/min, so scans can be averaged for several minutes.
- Stability is about 6 times better!

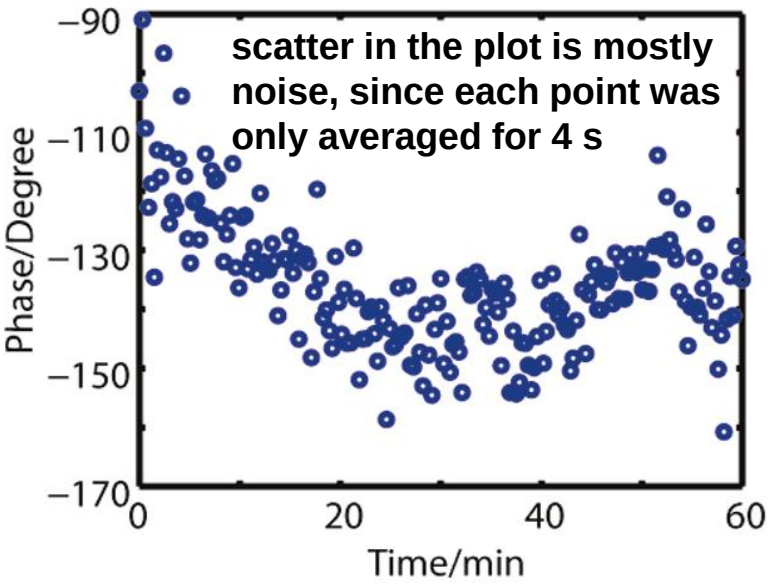

Balanced HD SFG signals in the frequency domain

- Ex: if a 50/50 beam splitter is used to combine LO and emitted field at a 90° angle, then the two measured signals

$$\left|E_{LO}+E^{(2)}\right|^2 = |E_{LO}|^2 + 2Re\left(E_{LO}^* E^{(2)}\right) + \left|E^{(2)}\right|^2$$
$$\left|E_{LO}-E^{(2)}\right|^2 = |E_{LO}|^2 - 2Re\left(E_{LO}^* E^{(2)}\right) + \left|E^{(2)}\right|^2$$

Subtract

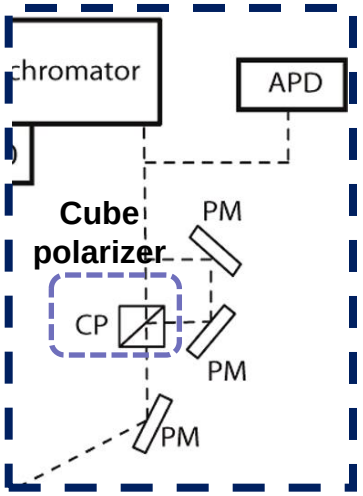

- Here, LO polarisation ⊥ to the desired signal and insert a CP after the sample oriented at 45° relative to the local oscillator and signal polarizations.
- So, LO and signal fields are projected onto two orthogonal polarization axes, which necessitates that their interference is 180° out-of-phase, as in eqs.

Balanced HD SFG signals in the frequency domain

- Ex: if a 50/50 beam splitter is used to combine LO and emitted field at a 90° angle, then the two measured signals

Subtract

$$\left|E_{LO}+E^{(2)}\right|^2=|E_{LO}|^2+2Re\left(E_{LO}^{*}E^{(2)}\right)+\left|E^{(2)}\right|^2$$

$$\left|E_{LO}-E^{(2)}\right|^2=|E_{LO}|^2-2Re\left(E_{LO}^{*}E^{(2)}\right)+\left|E^{(2)}\right|^2$$

- Here, LO polarisation ⊥ to the desired signal and insert a CP after the sample oriented at 45° relative to the local oscillator and signal polarizations.
- As a result, LO and signal fields are projected onto two orthogonal polarization axes, which necessitates that their interference is 180° out-of-phase, as in eqs.

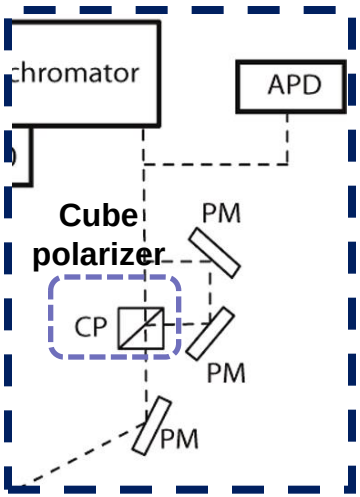

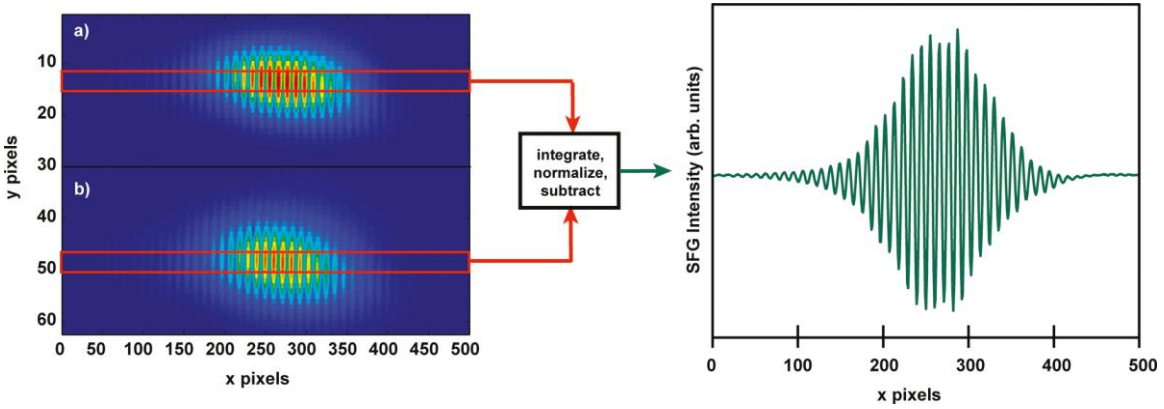

(a) Image of the interference pattern from beam transmitted through the polarizer,

(b) interference pattern from beam rejected by the polarizer,

(c) subtracted trace illustrating background cancellation

Phase Control with Mid-IR Pulse Shaping

Frequency-domain heterodyned signals obtained with phases of 0 (red, solid) and π (blue, dotted) applied to the IR pump pulse using the pulse shaper.

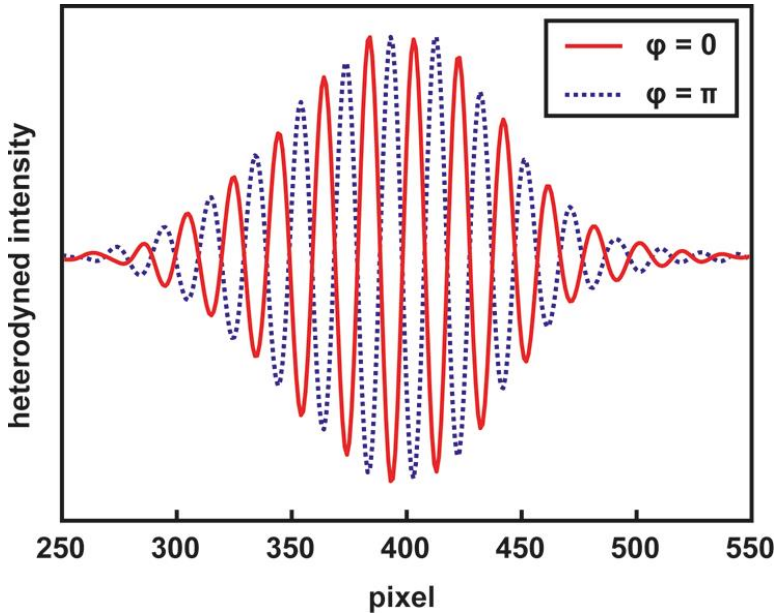

Time Domain in the Rotating Frame

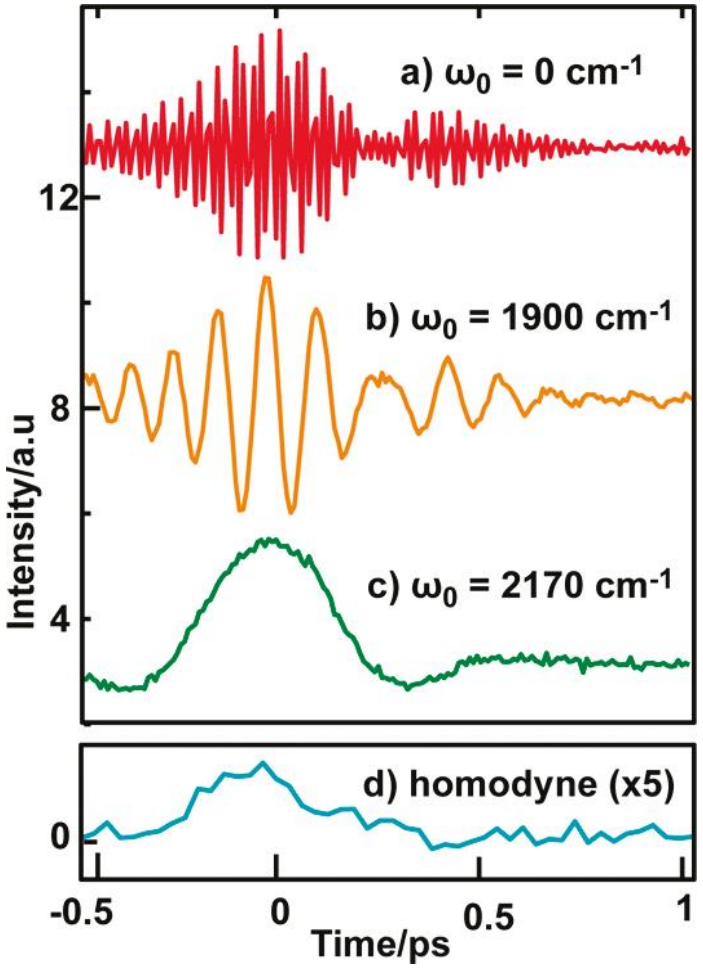

Measurements Results